Algorithm Theoretical Basis Document (ATBD) for Calibration of space sensors over Rayleigh Scattering : Initial version for LEO sensors

Bertrand Fougnie, Patrice Henry
CNES
2nd July, 2013

1. Introduction

The top-of-atmosphere (TOA) signal measured by a satellite sensor observing oceanic targets is in large proportion due to scattering of the incident solar irradiance by atmospheric components, especially in the visible. In this spectral range, the molecular scattering, co-called Rayleigh scattering, is the main process contributing to the TOA signal and this contribution can be accurately predicted and computed using surface pressure, knowing the spectral response of the instrument.

Other processes contributing to the TOA signal are aerosol scattering, back scattering by the water body, diffuse reflection by whitecaps, specular (or Fresnel) reflection by the surface, and gaseous absorption. Satellite acquisitions over such oceanic targets can be selected so that the contribution of these secondary processes is minimized. For these acquisitions, the molecular scattering signal may constitute as much as 90% of the TOA signal, for spectral bands from blue to red bands (typically 443 to 670nm). This forms the basis of the calibration method using Rayleigh scattering.

This method, derived from Vermotte et al. (1992), was previously explained in Hagolle et al. (1999). The approach is statistical, in the sense that climatology is used for marine reflectance, and that cases contaminated by aerosols (above a given background level) are rejected, i.e., the effect of aerosols require a very small correction. This contrasts with the vicarious radiometric calibration using in-situ measurements (see Section 4), in which the TOA signal is accurately computed using measurements of aerosol optical properties and water-leaving radiance. The advantage of the method using Rayleigh scattering is that the calibration is neither geographically or geo-physically limited, but it is derived from a large set of oceanic sites, from both hemispheres and for a large set of conditions.

Important comments regarding the GSICS framework :
Calibrate many sensors using the same Rayleigh scattering is a way to address the cross-calibration between these two sensors, as if it is not a direct cross-calibration technic. It can be seen as a double-difference approach over Rayleigh scattering. Depending on the accuracy that is needed, it will be mandatory to use the same Rayleigh scattering definition in the case of multiple implementations. This implies the use of the same radiative transfer codes to generate LUT, or, if not, to preliminarily document the possible biases between various radiative transfer codes, and their associated inputs.

The following algorithm is now fully mature for LEO sensors because it was operated for 15 years and over many sensors. It is pointed out some specificity for GEO sensors : for example a limited access to oceanic sites, and a specific viewing geometry for each sites…. As if

encouraging on-going developments have been made for SEVIRI, there is still not a significant feedback today for GEO sensors.

2. Selection of relevant pixels – The selection stream

Selection of relevant pixels is a crucial part of the performance of this method. It may sensitively impact the final result and strongly impact the behavior of results with various parameters. The basic goal is to select very clear pixels for which the assumption of a very dominant molecular scattering contribution will be relevant and for which secondary order contributions (surface, aerosol, gas) will remain small and will be considered with a sufficient precision.

• Step 1 : Geographical selection. The marine contribution represents 10 to 15% of the TOA signal for blue bands (but only a few percent for red bands) and is consequently an important source of error in attempting to meet the 1 or 2% accuracy on the TOA signal. A climatological study, based on analyzing one year of SeaWiFS data, was performed by Fougnie et al. (2002) to select adequate oceanic sites for which spatial homogeneity is guaranteed and for which moderate seasonal effects exist. This result was extended to a 9 years archive of SeaWiFS data in Fougnie et al. (2010). Using such pre-defined oceanic sites the dispersion of the results inside a given site is significantly reduced, as well as biases between results obtained over the different sites. In practice, six major oceanic sites were recommended by Fougnie et al. (2002 and 2010) in the North and South Pacific, the North and South Atlantic, and in the Indian oceans (see Table 1 and Figure 1).

Table and Figure 1. Major oceanic sites recommended for the statistical calibration method using Rayleigh scattering. (according Fougnie et al., 2002. and 2010.)

n°	Name	Location	Latitude (deg)		Longitude (deg)	
			min	max	min	max
1	PacSE	South-East of Pacific	-44.9	-20.7	-130.2	-89.0
2	PacNW	North-West of Pacific	10.0	22.7	139.5	165.6
3	PacN	North of Pacific	15.0	23.5	179.4	200.6
4	AtlN	North of Atlantic	17.0	27.0	-62.5	-44.2
5	AtlS	South of Atlantic	-19.9	-9.9	-32.3	-11.0
6	IndS	South of Indian	-29.9	-21.2	89.5	100.1

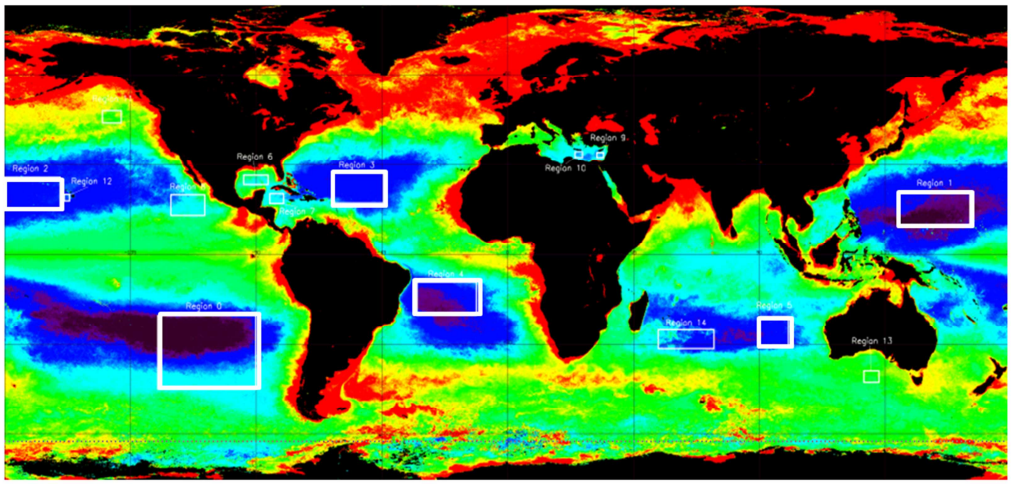

Note : in a refined analysis, some sub regions of these main sites may be ignored for some given months in the years, because of possible anomalies on the surface properties as reported in Fougnie et al. (2010).

• Step 2 : Rough cloud mask. A rough cloud mask can be made in order to limit the amount of data that will be processed in the following of the processing chain. It can be based on the level-1 cloud mask, when available, or using a simple threshold on a near infrared band (quite easy over ocean).

• Step 3 : Cloud mask dilatation. A dilatation of the previous cloud mask is made in order to discard all pixels that are located in the vicinity of clouds where we know adjacency effects are sensitive. An ideal distance of 30km from a cloud is recommended.

• Step 4 : Geometrical selection. Pixels potentially contaminated by sun glint are rejected. For that, all observations corresponding to viewing direction inside a cone of ±60° around the specular direction are discarded. This selection can be made using the wave angle, θ_n, that must be larger than 30°, and defined by (see Hagolle et al., 2004).

$$\theta_n = \arccos\left(\frac{\cos\theta_s + \cos\theta_v}{2\cos(\theta_p/2)}\right)$$

where θ_p is the phase angle, i.e. the angle between sun direction and satellite direction (θ_p= arccos (cos θ_s cos θ_v + sin θ_s sin θ_v cos (ϕ_s-ϕ_v))).
Additional selection can be added. Viewing and solar zenith angles can be limited up to 60° because of decreasing accuracy for larger airmass of radiative transfer codes used to predict the TOA signal.

• Step 5: Invalid ancillary data : Some exogenous data are mandatory for an accurate estimation of the TOA signal : surface pressure, surface wind speed, total column water vapor, ozone content must be valid.

• Step 6: Surface wind speed : Whitecaps appears on the sea surface when the wind speed reaches 7m/s and can becomes a great perturbation for large wind speeds. Consequently, pixels corresponding to surface wind speed larger than 5m/s (ideally) have to be discarded.

• Step 7: Quality index control : Pixels corresponding to inappropriate quality index are discarded. This quality index is sensor dependent and is taken from the corresponding fields in level-1 product.

• Step 8 : Turbid pixel rejection : A preliminary cloud mask was applied on step 2. A very strict threshold is applied here using a near infrared band (NIR_bd, usually around 865nm). Pixels corresponding to radiance(NIR_bd)xcos(θs)xcos(θv) larger than 0.003 are discarded (i.e. 3E-3). Using this threshold, it is possible to efficiently eliminate all situations corresponding to sub-pixel clouds, aerosol loads larger than the background level, undetected surface whitecaps, residual sunglint, unidentified floating object. This threshold is strict in order to limit the turbidity level to a level close to the background for which the following approach to model the TOA signal will stay accurate. The remaining mean level of aerosol is close to 0.05 in optical thickness (and less than 0.1).

3. Computation of the TOA reflectance

The following general formulation is used to compute the TOA signal (reflectance):

$$\rho_{TOA}(\theta_s, \theta_v, \phi) = t_g(\theta_s, \theta_v) \{ \rho_A(\theta_s, \theta_v, \phi) + \rho_w(\theta_s, \theta_v, \phi) T(\theta_s, \theta_v) / [1-S_A\rho_w(\theta_s, \theta_v, \phi)] \}$$

where θ_s, θ_v, and ϕ are the solar zenith, viewing zenith, and relative azimuth angles, respectively, t_g is the total gaseous transmittance, ρ_A is the molecular and aerosol contribution including coupling terms and specular reflection by the wavy surface, ρ_w is the marine reflectance, T is the total atmospheric transmission for aerosols and molecules, and S_A is the atmospheric albedo. Note that t_g depends on the amount of absorbers (essentially ozone), ρ_A on aerosol optical thickness, surface pressure, and wind speed, T on surface pressure and wind speed, and S_A on aerosol optical thickness. These different terms are evaluated as described below.

• Aerosol and molecular scattering contribution. The atmospheric functions ρ_A, T, and S_A are computed using an accurate radiative transfer model, such as the successive order of scattering code of Deuzé et al. (1989), or Lenoble et al. (2007). This code includes polarization and specular reflection by the wavy surface. The molecular scattering contribution is accurately computed knowing the surface pressure and the molecular optical thickness corresponding to the considered spectral band. For this, the Rayleigh equivalent optical thickness is calculated for a given spectral band by weighting the spectral optical thickness computed according to Gordon et al. (1988) by the spectral solar irradiance and the spectral response within the band. The background aerosol contribution is computed knowing its optical thickness estimated at 865nm (or another reference band) and extrapolated for the considered spectral band using a Maritime 98 aerosol model (Gordon and Wang, 1994). In practice, the restrictive thresholds defined in section 2 and used for the clear pixel selection lead to a residual aerosol optical thickness lower than 0.05 at 865nm, and usually about 0.02-0.035.

• Marine contribution. This contribution, representing about 10% of the TOA signal for shorter wavelengths, is estimated over the pre-defined oceanic sites through a climatological study (Fougnie et al., 2002). The typical marine reflectance for these sites is 0.033 at 443nm, 0.020 at 490nm, 0.0049 at 555nm, and 0.0007 at 670nm, and is close to values derived through a bio-

optical model using a surface pigment concentration of 0.07 mg/m^3. A spectral interpolation can be performed when the spectral band of interest is not exactly the same as one of the SeaWiFS spectral bands for which the climatological values are available. In addition, a bi-directional correction is added as an option in order to take into account sensible differences in the viewing and solar geometries of the pixel to calibrate and the angular conditions of the climatological values derived from SeaWiFS (e.g., due local time of overpass or case of multi-directional viewing sensors). This correction is made according to Morel et Gentili (1993).

• Gaseous contribution. A gaseous absorption is effected for each spectral band. The main contributors are water vapor (mainly around 565 and 865nm), ozone (mainly around 490, 565, and 670 nm), oxygen (around 765 nm), nitrogen dioxide (mainly around 443 and 490 nm). The correction is made according to the SMAC model (Rahman and Dedieu, 1994) using exponential variation with air mass and gaseous amount.

4. Sampling

The evaluation consists in comparing the TOA normalized radiance computed with the radiative transfer model (CI) with the normalized radiance derived from the sensor measurements (MI), assuming a given calibration (the one we want to evaluate). Consequently, the ratio ΔA_k, defined as MI / CI, provides a measure of the bias in calibration coefficients with respect to reference values. This comparison is made for each selected pixel and/or viewing direction.

It was evidenced that a site by site analysis is sometimes useful. In fact, residual biases still exist on the knowledge of marine reflectance and these biases differ for each oceanic site. If we limit the analysis to one given site, the bias will be the same for each pixel of the data set, and some particular relative effects (of course not absolute), such as a small temporal decrease or multi-angular calibration errors, become easier to detect.

The analysis with other various parameters can help with understanding potential problems. For example, the variation with viewing geometry (zenith viewing angle for instance) may indicate some problem in the multi-angular calibration, called sometimes the smile effect. The variation with aerosol content may reveal a problem in the calibration of the 865nm spectral band (or the spectral band used to estimate the aerosol amount), or on the supposed aerosol model (Maritime 98). The variation with the Rayleigh contribution or with geometry may point to some residual problem with the polarization sensitivity of the instrument.

5. Error budget elements

Table 2 summarizes a first realistic error budget of the method. For this budget, we have estimated the impact on calibration results of typical uncertainties on the input parameters. We have considered errors made on the surface pressure and surface wind speed (impacting the Rayleigh contribution), on the calibration of the 865nm band and on the expected aerosol model

(impacting the aerosol contribution), on the gaseous absorption, and on the marine reflectance. In this error budget evaluation, using the root-mean-squared (RMS) error as a measure of performance is appropriate and realistic, because of the large amount of data considered in the synthesis, i.e., several geometric, geographic, and geophysical conditions.

In general, the error budget, in terms of RMS, is less than 3.5%. For shorter wavelengths, 443, 490, and 510 nm, the performance is determined by the accuracy on the marine reflectance. This confirms the interest of and justifies using in some cases the complementary vicarious approach based on in-situ measurements to improve the accuracy of the statistical results. For wavelengths near 565nm, the performance depends quite equally on the errors of all the parameters. In the red, i.e., 670nm, error in the calibration in the near infrared (865 nm) becomes the limiting factor to accuracy.

This error budget is being consolidating and an updated version will be released as soon as possible.

Table 2. Typical error budget for the 6 main sources of uncertainties.

Error (in %)	443	490	510	565	670
surface pressure : 10hPa	0.81	0.81	0.81	0.81	0.82
surface wind speed : 2m/s	0.15	0.26	0.30	0.40	0.51
calibration at 865 : 3%	0.50	0.40	0.49	0.74	1.42
aerosol model (50% a 443)	0.57	0.55	0.53	0.42	0.33
gas amount error of 20%	0.12	0.38	0.71	1.62	0.74
marine reflectance	3.06	2.59	2.16	0.96	0.33
RMS	3.26	2.84	2.53	2.25	1.93
MAX	5.21	4.99	4.99	4.94	4.14

6. Examples

The following examples were produced using exactly the same algorithm implemented at CNES in the MUSCLE/SADE environment.

Figure 3. Validation of the calibration of red bands versus observed normalized radiance

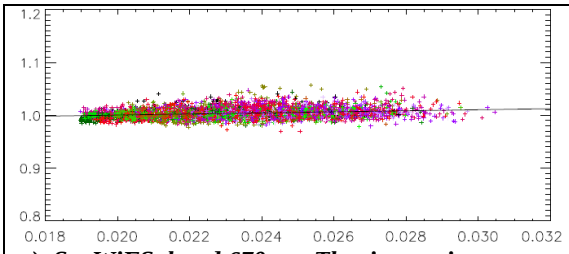

a) SeaWiFS, band 670nm. The time series covers year 1998. (mean=1.004, stdev=0.9%)

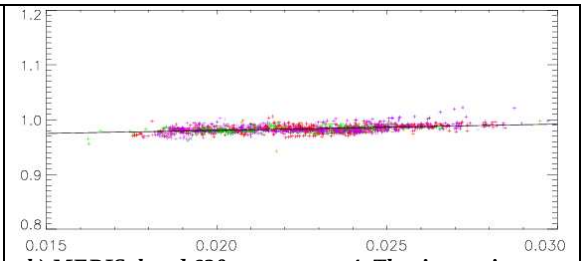

b) MERIS, band 620nm, camera-4. The time series covers year 2010. (mean=0.983, stdev=0.6%)

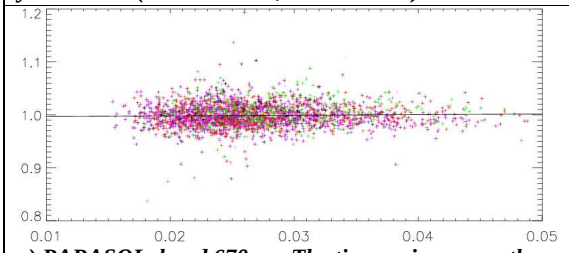

c) PARASOL, band 670nm. The time series covers the 2005-2007 period. (mean=0.998, stdev=2.1%)

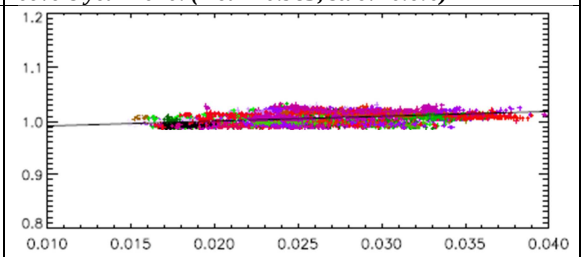

d) MODIS, band 667nm. The time series covers december2005. (mean=1.004, stdev=1.0%)

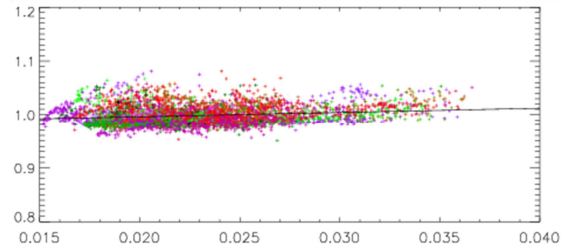

e) VEGETATION-2, band 670nm (B2). The time series covers May2011. (mean=0.998, stdev=1.8%)

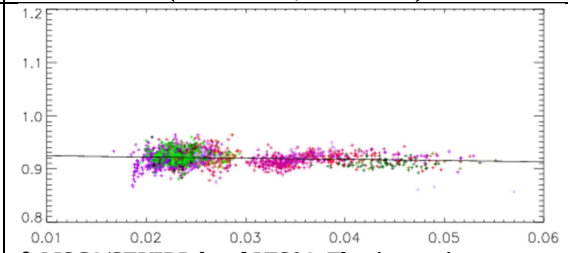

f) MSG2/SEVIRI, band VIS06. The time series covers the 2009-2010 period. (mean=0.92, stdev=1.3%)

7. References

Deuzé, J.-L., M. Herman, and R. Santer, Fourier series expansion of the transfer equation in the atmosphere-ocean system, *J. Quant. Spectrosc. Radiat. Transfer*, **41**, pp. 483-494, 1989.

Fougnie, B., G. Bracco, B. Lafrance, C. Ruffel, O. Hagolle, and C. Tinel, PARASOL In-flight Calibration and Performance, *Applied Optics*, vol. 46, N° 22, pp. 5435-5451, 2007.

Fougnie, B., P. Henry, A. Morel, D. Antoine, and F. Montagner, Identification and Characterization of Stable Homogeneous Oceanic Zones : Climatology and Impact on In-flight Calibration of Space Sensor over Rayleigh Scattering, *Proceedings of Ocean Optics XVI*, Santa Fe, New Mexico, 18-22 November, 2002.

Fougnie B., P. Henry, S. Lachérade, P. Gamet, D. Jolivet, B. Lafrance, V. Bruniquel, G. Fontanilles, L. Bourg, L. Gross-Colzy, "In-Flight Calibration of Space Sensors Through Common Statistical Vicarious Methods : Toward an Ocean Color Virtual Constellation," *Ocean Optics XXI*, Glasgow, Scotland, 8-12 October, 2012.

Fougnie B., J. Llido, L. Gross-Colzy, D. Blumstein, and P. Henry, Climatology of Oceanic Zones Suitable for In-flight Calibration of Space Sensors, *Earth Observing Systems XV*, SPIE Optics & Photonics, San Diego, California, 1-5 August, 2010.

Gordon, H. R., and M. Wang, Retrieval of water-leaving radiance and aerosol optical thickness over the oceans with SeaWiFS: a preliminary algorithm, *Appl. Opt*., **33**, pp. 443-452, 1994.

Gordon, H. R., J. W. Brown, and R. H. Evans, Exact Rayleigh scattering calculations for use with the Nimbus-7 Coastal Zone Color Scanner, *Appl. Opt*., **27**, pp. 862-871, 1988.

Hagolle, 0., P. Goloub, P.-Y. Deschamps, H. Cosnefroy, X. Briottet, T. Bailleul, J.M.Nicolas, F. Parol, B. Lafrance, and M. Herman, Results of POLDER In-Flight Calibration, *IEEE Trans. on Geosci. Remote Sensing*, vol. 37, pp. 1550-1566, 1999.

Hagolle, O., J.M. Nicolas, B. Fougnie, F. Cabot, and P. Henry, Absolute Calibration of VEGETATION derived from an interband method based on the Sun Glint over Ocean, *IEEE Trans. Geosci. and Remote Sensing*, vol. 42, No.7, pp. 1472-1481, 2004.

Lenoble J., M. Herman, J.L. Deuze, B. Lafrance, R. Santer, D. Tanre, "A successive order of scattering code for solving the vector equation of transfer in the earth's atmosphere with aerosols", Journal of Quantitative Spectroscopy & Radiative Transfer 107, 479-507, 2007.

Morel, A., and B. Gentili, Diffuse reflectance of oceanic waters (2): Bi-directional aspects., *Appl. Opt*., **32**, pp. 6864-6879, 1993.

Rahman, H., and Dedieu, G, SMAC: a simplified method for the atmospheric correction of satellite measurements in the solar spectrum. *Int. J. Remote Sensing*, **15**, pp. 123-143, 1994.

Vermote, E., R. Santer, P.-Y. Deschamps, and M. Herman, In-flight calibration of large field of view sensors at shorter wavelengths using Rayleigh scattering*, Int. J. Remote Sensing*, vol. 13, pp. 3409-3429, 1992.

8. Summarized Version of the ATBD